Sigma Journal of Engineering and Natural Sciences
Web page info: https://sigma.yildiz.edu.tr
DOI: 10.14744/sigma.2023.00101

Research Article

Influence of burnishing process on surface integrity of inconel 718 fabricated by laser powder bed fusion additive manufacturing

Mert KAYA[1,*], Nihal YAMAN[2], Emre TAŞCIOĞLU[3], Yusuf KAYNAK[2]

[1]Department of Mechanical Engineering, Piri Reis University, Istanbul, 34940, Türkiye
[2]Department of Mechanical Engineering, Marmara University, İstanbul, 34722, Türkiye
[3]Torun Metal, R&D Center, Kocaeli, 41400, Türkiye

ARTICLE INFO

Article history
Received: 14 March 2022
Revised: 06 June 2022
Accepted: 04 April 2023

Keywords:
Additive Manufacturing; Surface Integrity; Roller Burnishing

ABSTRACT

This present study aims to contribute to the literature in understanding the roles of roller burnishing parameters and conditions on Inconel 718 alloy fabricated by Laser Powder Bed Fusion (LPBF). The roller burnishing process was performed with three burnishing forces (300 N, 600 N, 900 N) and under three cooling conditions (namely cryogenic, dry, and preheat). The effects on surface integrity characteristics including surface roughness, microstructure, microhardness, and XRD were investigated. The results illustrate that the burnishing force remarkably influences the decrease the surface roughness under all burnishing conditions. It was possible to reduce the surface roughness from 23 µm to 0.794 µm after turning applied to the as-built part followed by roller burnishing with 900N under dry conditions. When the microstructures were examined, the roller burnishing process caused plastic deformations and reductions in grain sizes. It was observed that the affected layer depth could reach 4.3 µm with 900N under preheat conditions. With the roller burnishing process, it was possible to increase the surface microhardness by 21% depending on the parameter and condition. The roller burnishing process had notable effects on XRD patterns of Inconel 718 alloy fabricated by LPBF.

Cite this article as: Kaya M, Yaman N, Taşcıoğlu E, Kaynak Y. Influence of burnishing process on surface integrity of inconel 718 fabricated by laser powder bed fusion additive manufacturing. Sigma J Eng Nat Sci 2024;42(2):335–343.

INTRODUCTION

Inconel 718 is a material found in the group of nickel-chromium-based super alloys, with high yield and tensile strength, high creep resistance, high oxidation and corrosion resistance and it shows good behavior against extremely demanding conditions such as high pressure and temperature [1-4]. Due to these properties, Inconel 718 is widely used in aerospace, defense industry, automotive and energy sectors, etc. [5, 6]. Machining, which is one of the traditional manufacturing methods, is widely used in the shaping of Inconel 718. However, machining of this alloy seems difficult because it causes micro-welding and stacked edge formation at the tooltip and chip interface [7]. It is also classified as "hard-to-cut materials" [8]. This situation

*Corresponding author.
*E-mail address: amamertkaya@gmail.com

This paper was recommended for publication in revised form by Regional Editor in Cheif Ahmet Selim Dalkilic

paved the way for the additive manufacturing method, which has recently become widespread and is widely used in many industries. Additive manufacturing has a unique advantage such as high geometric complexity, reduction of production steps, low material consumption, reduction of lead time, and low production cost [9-11]. LPBF, one of the additive manufacturing methods, is widely used in the production of Inconel 718 [12]. But it also has some disadvantages like surface roughness, tensile residual stress, porosity, and cracks [13-15]. First of all, it is aimed to eliminate or reduce these disadvantages with production parameter optimization. Even in productions carried out at optimum parameters, surface quality, and mechanical properties may not be at the desired level. This situation makes post-processing necessary [16]. Post-processes are selected according to the material used, the desired mechanical properties, and surface quality. Roller burnishing is an easy-to-use, cost-effective post-process that creates compressive residual stress on the part surface as well as increasing the surface quality [17]. In the literature, Raaj et al. [18] applied low plasticity burnishing post-processing at different pressures (10, 20, 30, 40 MPa) after grinding to Inconel 718 material produced by electron beam additive manufacturing. They reported that at the highest pressure, the surface hardness increased by 25%, the porosity decreased by 89%, the surface roughness decreased by 99%, and a compressive residual stress of 1300 MPa occurred on the surface. Yaman et al. [19], we applied a roller burnishing process with two burnishing conditions (dry, air), with two burnishing forces (250, 750 N) and two burnishing speeds (350, 1050 RPM) to as built, sandblasted, and heat treated Inconel 718 parts manufactured with LPBF. As a result, the lowest surface roughness was achieved after sandblasting + roller burnishing post-processing with a decrease of 98%, and the highest wear resistance on the surface was 55% after heat treatment + roller burnishing. Shinoda et al. [20] reported that after preheating at 200°C on the Inconel 718 part produced with LPBF, the creep life of the part increased by 2.09 times and the lower creep elongation increased by 1.4%. Yıldırım et al. [21] turned Inconel 625 in different cutting environments such as dry, minimum amount of lubrication, nanofluids, cryogenic cooling, and combinations of these cooling methods. They reported that the best results were cryogenic with nano-fluid technique to improve turning performance in the results evaluated according to tool-chip interface temperature, surface roughness, and tool wear.

In this study, roller burnishing was applied to Inconel 718 parts fabricated by LPBF under different conditions after turning. The roller burnishing process was performed at 300 N, 600 N, and 900 N burnishing forces under dry, preheated at 200°C and cryogenic burnishing conditions. The effects of these conditions on the surface roughness, microhardness, and microstructure were examined and XRD measurements were presented. Also, it is aimed to reveal the effect of severe plastic deformation on surface integrity, which occurs because of roller burnishing under different conditions applied to Inconel 718 parts produced with LPBF.

MATERIALS AND METHODS

Material and Material Manufacturing Parameters

In this study, Ø20 x 80 mm Inconel 718 nickel-based super alloy cylinders produced by LPBF process on ENAVISION 250 3D Additive Manufacturing Machine were used. Process parameters are presented in Table 1. In this machine, these production parameters are the optimum production parameters determined for Inconel 718 [19, 22].

Table 1. Parameter set used in the manufacturing of specimens by LPBF method

Laser Spot Diameter, d (μm)	85
Laser Scanning Speed, v (mm/s)	700
Laser Power, P (W)	190
Hatch Distance, h (μm)	70
Layer Thickness, t_{layer} (μm)	20
Recoater Time, (s)	11
Scanning Strategy	Chessboard (5x5 mm)
	Strip Rotate 67° Pattern
Base Plate Material	S316L

CNC Turning, Roller Burnishing, and Heat Treatment Processes

The cylinder specimens were machined on a Doosan Puma GT2100 CNC turning center before the roller burnishing process was applied. DNMG 11 04 04-MF 1105 coated carbide tools used in machining and the cutting speed was 60 m/min, the depth of cut (αp) 0.2 mm, feed rate (f) 0.1 mm/rev, under dry burnishing condition.

After turning, in the turning direction, the roller burnishing process was applied under three different burnishing forces and three burnishing conditions. The parts were heated to 200°C with using a 7-step programable furnace capable of reaching high temperatures (0-1200°C), and 5000 W power (23 A/Phase) under the atmosphere. Then they were roller burnished with 300 N, 600 N, and 900 N burnishing forces (Figure 1(a).). The same procedures were repeated for the dry parts at room temperature. In addition, these processes were repeated by cooling with liquid nitrogen during the process to reveal the effect of cryogenic conditions on burnishing (Figure1(b).). Other burnishing parameters are taken as constant throughout the process; the burnishing speed was 30 m/min, the feed rate was 0.1 mm/rev. For the roller burnishing operations, YAMASA SX8 single-ball roller burnishing tool was used. Roller

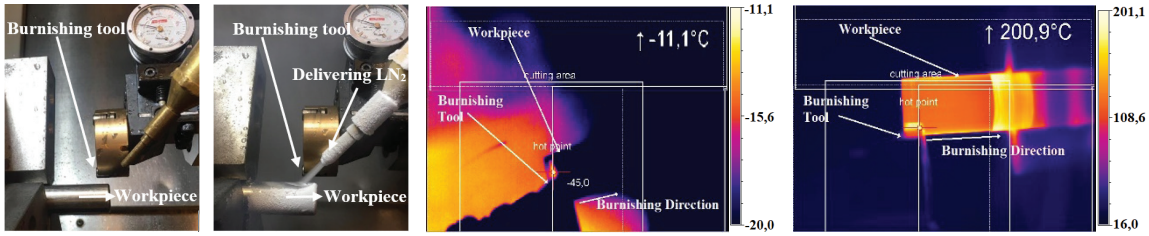

(a) (b) (c) (d)

Figure 1. Roller burnishing process (a) dry condition, (b) cryogenic condition and (c) cryogenic condition with infrared camera image of -11°C (d) preheat condition with infrared camera image of 200°C.

burnishing forces were determined by deducting a certain ratio from the maximum force to be applied to Inconel 718 for the selected roller burnishing tool.

Optris Infrared Camera

Temperature measurements during the roller burnishing process were made with the Optris PI 400 infrared camera with ±2% sensitivity and a resolution of 329x288 pixels. A sample was raised to a constant temperature using an oven, and the accuracy of the temperature was confirmed by measuring with both a thermocouple and a camera at the same time. As a result of calibration, the emissivity value was found to be 0.67 and was applied for temperature measurement. Figure 1(c) shows the infrared camera image taken while roller burnishing is applied to the part where the ambient temperature is -11 °C in the cryogenic condition and the part temperature drops to -45 °C. Figure 1(d) shows the infrared camera image taken while roller burnishing is applied to the piece heated to 200°C in the oven.

Characterization of Samples

A 3D Keyence VHX-6000 optical microscope was used to examine the surface topography, surface roughness, and microstructure of etched parts. To examine the surface and subsurface layer after the roller burnishing process, parts were cut with a diamond cutting disk followed by cold-mounted, ground, and polished. The Bruker Smart Apex II Quazar X-Ray Single Crystal Diffraction Device was used for the X-ray diffraction (XRD) measurements of the polished parts. Cu Kα cathode with a wavelength of 1.54 *A* was used in XRD measurements carried out within the scope of phase analysis, and the current and voltage values were chosen as 40 mA and 40 kV, respectively. The polished surface was etched using a solution of 15 ml HCl, 10 ml Glycerol, and 5 ml HNO_3 to review the microstructure. Etched parts were also examined with the FEI (PHILIPS) XL30 SFEG SEM scanning electron microscope. Future-Tech FM310e device was used for hardness measurements. The hardness of each part was determined following the ASTM E 384 standard with an average of 5 measurements, a load residence time of 15 s, and a test load of 100 gf.

RESULTS AND DISCUSSIONS

Surface Roughness

The surface roughness of the Inconel 718 parts manufactured with LPBF was measured Sa=23 µm and Sz=177.69 µm after production. With the turning parameters given in the experimental procedure, the surface roughness of the parts reduced to Sa=1.7 µm and Sz=23.75 µm. Both the turning process and the roller burnishing process were carried out in parallel with the build direction. In Figure 2 the surface roughness values obtained as a result of the different processes applied in this study are shown. It was observed that the surface roughness decreased as the burnishing force increased on the roller-burnished surface under all burnishing conditions. The highest decrease in surface roughness was measured after the roller burnishing process performed at 900 N and dry conditions. Surface roughness values measured as Sa= 0.794 µm and Sz= 6.458 µm. As the burnishing force increased, the penetration depth of the process on the surface increased, which resulted in the flattening of the surface [23]. When the burnishing conditions are examined between each other, the surface roughness of the workpiece in the cryogenic burnishing condition is higher than the other conditions. Surface roughness was measured as Sa=1.012 µm and Sz=12.294 µm after the roller burnishing process was applied with 300 N burnishing force under cryogenic burnishing conditions. The reason for this is that the workpiece undergoes maximum plastic deformation with cryogenic burnishing, and as a result, it becomes difficult to machining, causing the surface roughness to be higher compared to other burnishing conditions [24]. For a similar reason, a better surface roughness was obtained compared to dry cutting conditions, since the preheat conditions applied to the part facilitate the machinability of the part.

Microstructure

The roller burnishing process causes plastic deformations, reductions in grain sizes, and orientations near the surface of the part [25]. Figure 3. shows the SEM photographs of the post-production state and turned Inconel 718 parts produced with LPBF parts at the same magnification. The microstructure on the surface and below is similar. Also, in the turned part no orientation or grain reduction

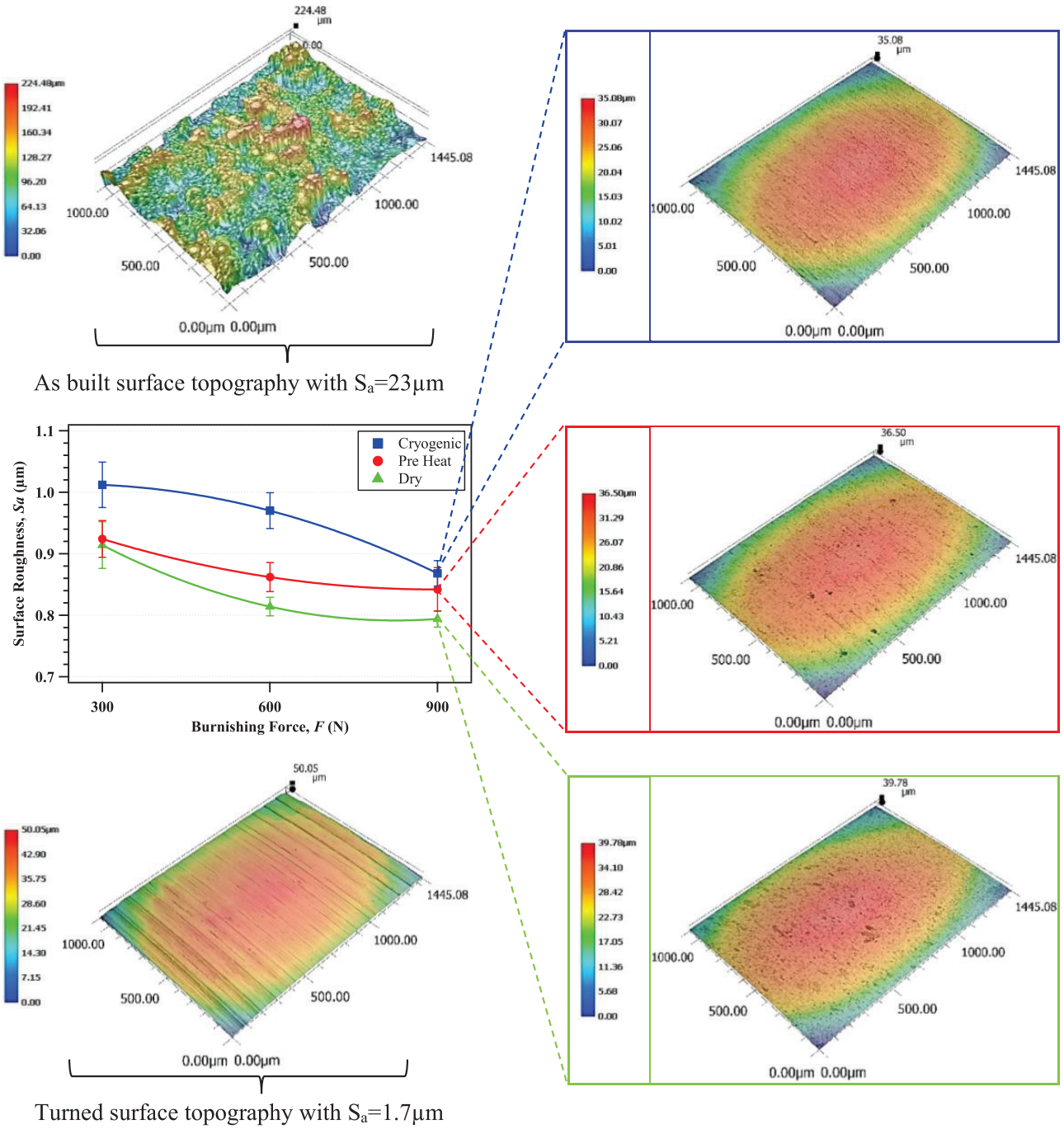

Figure 2. Surface roughness values of LPBF Inconel 718 parts with roller burnishing process applied in different parameters and topography images.

was observed. In Figure 4. a reduction in grain size is clearly seen on all surfaces after the roller burnishing process was applied. Grain size reduction increases the grain boundary area per unit volume. This means more grain boundary slippage and contributes to the overall deformation. The grain size reductions on the surface are clearly visible in the microstructures. The increase in plastic deformation due to these reductions can be explained as the reason for the increase in surface hardness [23]. As a result of detailed characterization on the surface after the roller burnishing process, a thin layer of white color was observed. Studies in the literature have shown that this structure is a deformed ultra-fine-grained or nanocrystalline structure [26]. In the roller burnishing process, it was observed that the affected layer thickness increased with the increase of the burnishing force. After roller burnishing was applied with a force of 300 N under cryogenic conditions, the affected layer was measured at about 2 µm. When the force was increased to

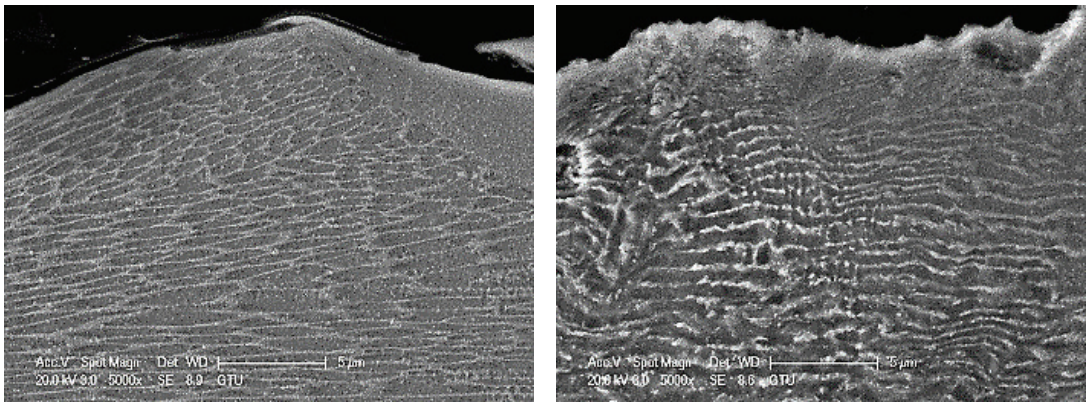

(a) (b)

Figure 3. SEM images of (a) as built and (b) turned LPBF Inconel 718 parts.

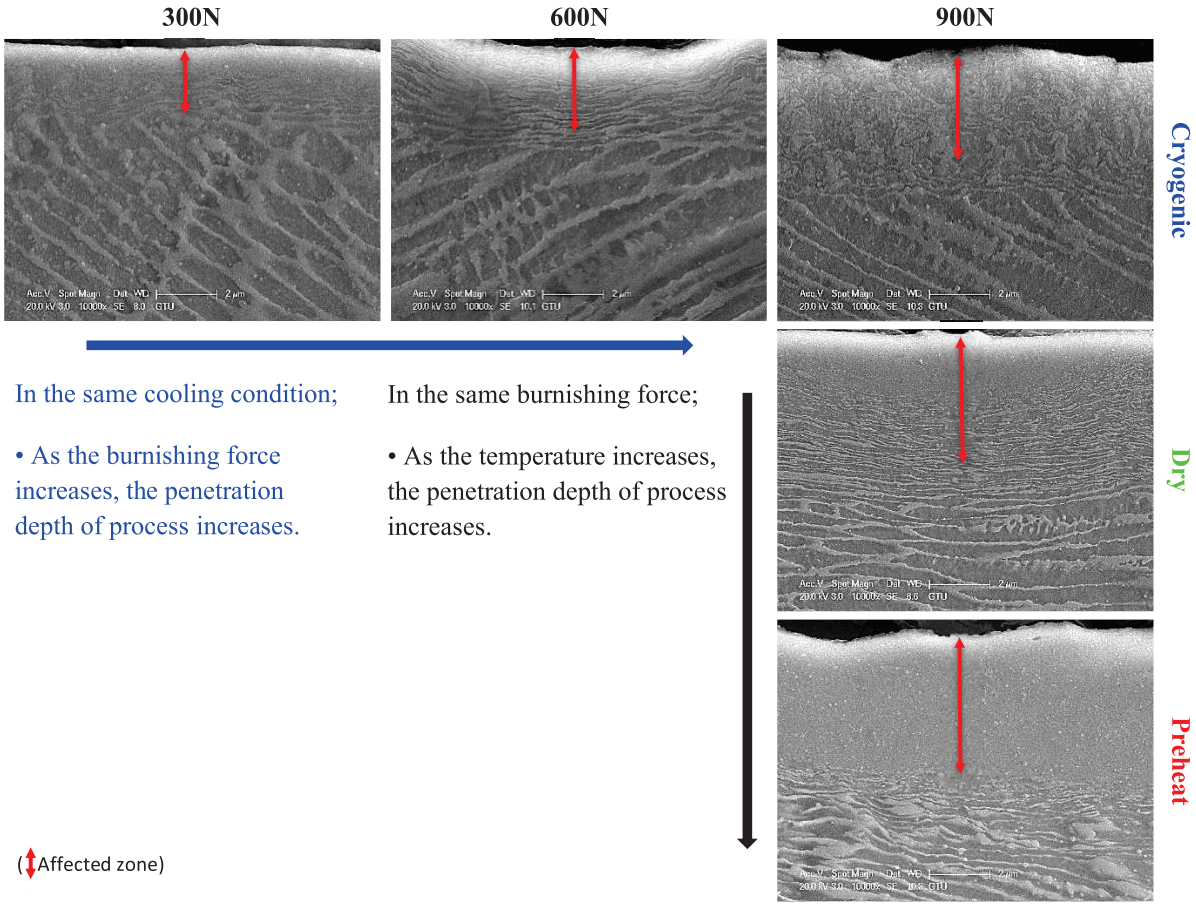

Figure 4. SEM images of roller burnished parts with different burnishing forces and different burnishing conditions.

900 N, the affected layer increased to 3.3 μm. The reason for this is that the area undergoing permanent plastic deformation increases with the increase of forces exceeding the yield point of the material [27, 28].

When the SEM images were examined after the roller burnishing process performed with the same burnishing force under different burnishing conditions, it was observed that the depth of the part affected by the process increased as the temperature increased. While the affected layer depth as a result of roller burnishing performed at 900 N and cryogenic conditions was 3.3 μm, this value increased to 4 μm when performed under dry conditions with the same force. When the same process was applied to the preheated part, the affected layer depth increased to

4.3 μm. This is because the energy transfer between atoms under the preheat burnishing condition is greater than under other burnishing conditions. Thus, while the force applied to the heated part acts more deeply, it affects a lesser area under the cryogenic burnishing condition. Since the same force will act on less area, the plastic deformation on the surface of the workpiece is more under the cryogenic burnishing condition [29]. As a matter of fact, microhardness values confirm this.

Microhardness

After the roller burnishing process, the hardness values of the parts increased significantly. Figure 5. shows the microhardness values classified according to the applied burnishing forces. The microhardness of the as-built parts was measured at 352 HV. It was observed that the microhardness increased as the burnishing force increased under all burnishing conditions in the process performed with different burnishing forces. Considering the microhardness values measured at a depth of 15 μm from the surface, the hardest surface was obtained under cryogenic burnishing condition. The reason for this the burnishing force applied to the workpiece under the cryogenic burnishing condition acts on a smaller area resulting in a higher dislocation density [30]. Surface microhardness was measured at 428 HV after the roller burnishing process was applied with 900 N burnishing force under cryogenic burnishing condition. However, as can be seen from the SEM images, the penetration depth of the roller burnishing process is highest under preheat burnishing conditions, followed by dry and cryogenic conditions.

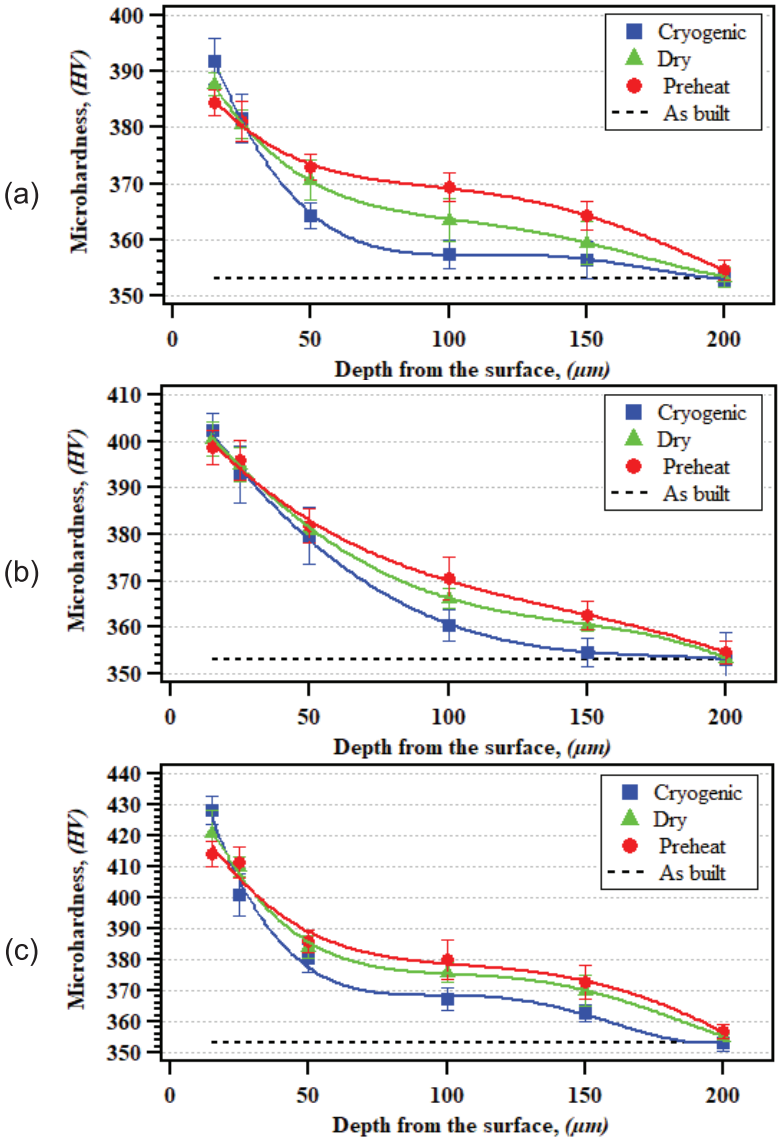

Figure 5. Microhardness values of LPBF Inconel 718 parts with roller burnishing process applied in (a) 300 N (b) 600 N and (c) 900 N burnishing forces.

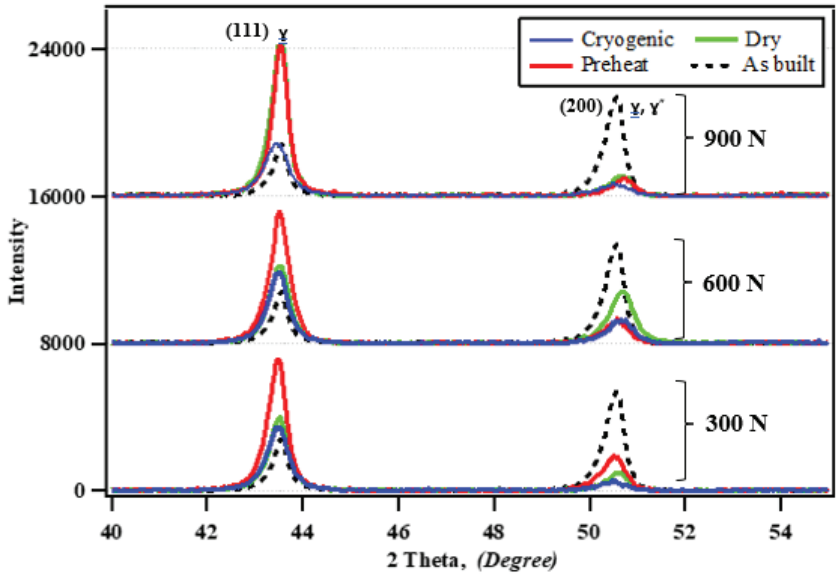

Figure 6. XRD results of roller burnished LPBF Inconel 718.

Although the penetration depth is the highest in the process performed under the preheat condition, the microhardness value on the surface is the lowest. The reason for this is that the material is more ductile under the preheated condition. Therefore, the area affected by the burnishing force acting on the unit area increases and the microhardness value on the surface decreases. Also, the annihilation and recovery of plastic deformation occurred due to high temperature [30, 31]. Surface microhardness was measured 385 HV after roller burnishing process applied with 300 N burnishing force under preheat condition.

XRD RESULTS AND DISCUSSION

Although the roller burnishing operation applied to the parts did not cause a new phase formation, it was observed that it caused a change in the widths and intensities of the peaks in the (111) and (200) planes. In addition, shifts were observed in the peak angles. Figure 6. shows the XRD results of roller-burnished LPBF Inconel 718 parts under 300 N, 600 N, and 900 N burnishing forces and preheat, dry, and cryogenic burnishing conditions.

The difference is most pronounced between the (111) and (200) planes. While as built has larger intensity at (200) plane, all roller burnished has larger intensity at (111) plane. When the (111) plane is examined, higher intensity and wider peaks are seen compared to the as-built one. Wider ɣ peaks indicate smaller grain structures [32]. The reason for the increase in the peak width is the grain reduction due to the increase in the force acting between the roller burnishing tool and the surface of the part when the force is high [33]. Increasing grain size is associated with microhardness.

CONCLUSION

This study presents the effect of the roller burnishing process with various parameters and under various conditions applied to Inconel 718 parts manufactured with LPBF. The following can be concluded from the present study;

- The roller burnishing process used after turning is a very effective post-processing operation to decrease surface roughness for the Inconel 718 parts manufactured with LPBF. Depending on the burnishing force, the surface roughness can be lowered between 46% and 54% under dry conditions.
- It has been observed that as the temperature of the treated part increases, which depends on roller burnishing conditions, the depth of the affected layer increases. As a matter of fact, the deepest affected layer was detected after the process carried out under the preheat burnishing condition. In this condition, at 900N burnishing force, the affected layer depth was 4.3 μm.
- The increase in roller burnishing force caused an increase in surface microhardness under all roller burnishing conditions. The hardest surface was obtained under the cryogenic burnishing condition, which increased by 21% compared to the as-built state.
- From the XRD pattern of Inconel 718 parts manufactured with LPBF, it has been observed that the burnishing force and burnishing conditions remarkably affect intensity at (111) and (200) planes. The roller burnishing process with 900N under preheat conditions resulted in an increase in the intensity of the (111) plane by up to 28% compared to the plane of the as-built state.

ACKNOWLEDGEMENTS

Financial support from TUBITAK (The Scientific and Technological Research Council of Turkey) under Project number 118R039 is greatly acknowledged.

AUTHORSHIP CONTRIBUTIONS

Authors equally contributed to this work.

DATA AVAILABILITY STATEMENT

The authors confirm that the data that supports the findings of this study are available within the article. Raw data that support the finding of this study are available from the corresponding author, upon reasonable request.

CONFLICT OF INTEREST

The author declared no potential conflicts of interest with respect to the research, authorship, and/or publication of this article.

ETHICS

There are no ethical issues with the publication of this manuscript.

REFERENCES

[1] Anderson M, Thielin A-L, Bridier F, Bocher P, Savoie J. δ Phase precipitation in Inconel 718 and associated mechanical properties. Mater Sci Eng A 2017;679:48–55. [CrossRef]

[2] Slama C, Abdellaoui M. Structural characterization of the aged Inconel 718. J Alloys Compd 2014;306:277–284. [CrossRef]

[3] Li R, Yao M, Liu W, He X. Isolation and determination for δ, γ′ and γ ″phases in Inconel 718 alloy. Scr Mater 2002;46:635–638. [CrossRef]

[4] Ergene B. Simulation of the production of Inconel 718 and Ti6Al4V biomedical parts with different relative densities by selective laser melting (SLM) method. J Fac Eng Archit Gazi Univ 2022;37:469–484. [CrossRef]

[5] Baicheng Z, Xiaohua L, Jiaming B, Junfeng G, Pan W, Chennan S, et al. Study of selective laser melting (SLM) Inconel 718 part surface improvement by electrochemical polishing. Mater Des 2017;116:531–537. [CrossRef]

[6] Kaynak Y, Tascioglu E. Post-processing effects on the surface characteristics of Inconel 718 alloy fabricated by selective laser melting additive manufacturing. Prog Addit Manuf 2019:1–14. [CrossRef]

[7] Feyzi T, Safavi SM. Improving machinability of Inconel 718 with a new hybrid machining technique. Int J Adv Manuf Technol 2013;66:1025–1030. [CrossRef]

[8] Sugihara T, Enomoto T. High speed machining of Inconel 718 focusing on tool surface topography of CBN tool. Procedia Manuf 2015;1:675-682. [CrossRef]

[9] Nguyen QB, Nai MLS, Zhu Z, Sun C-N, Wei J, Zhou W. Characteristics of inconel powders for powder-bed additive manufacturing. Engineering 2017;3:695–700. [CrossRef]

[10] Popovich V, Borisov E, Popovich A, Sufiiarov VS, Masaylo D, Alzina L. Impact of heat treatment on mechanical behaviour of Inconel 718 processed with tailored microstructure by selective laser melting. Mater Des 2017;131:12–22. [CrossRef]

[11] Yalçın B, Ergene B. Metallurgy and method of new trend 3-D additive manufacturing in industry. Uluslararası Teknolojik Bilimler Dergisi 2017;9:65–88.

[12] Mostafa A, Picazo Rubio I, Brailovski V, Jahazi M, Medraj M. Structure, texture and phases in 3D printed IN718 alloy subjected to homogenization and HIP treatments. Metals 2017;7:196. [CrossRef]

[13] Serrano-Munoz I, et al. The residual stress in as-built Laser Powder Bed Fusion IN718 alloy as a consequence of the scanning strategy induced microstructure. Sci Rep 2020;10:1–15. [CrossRef]

[14] Mert K, Sunay N, Kaynak Y. Comparison of finite element and empirical model prediction of surface residual stress in inconel 718 parts fabricated by laser powder bed fusion additive manufacturing. J Addit Manuf Technol 2021;1:592.

[15] Bandyopadhyay A, Bose S. Additive manufacturing. CRC Press; 2019. [CrossRef]

[16] Sunay N, Mert K, Kaynak Y. Chemical post-processing methods for enhancing surface properties of parts fabricated by additive manufacturing: a review. Sigma J Eng Nat Sci 2020;38:2027–2042.

[17] El-Axir M. An investigation into roller burnishing. Int J Mach Tools Manuf 2000;40:1603–1617. [CrossRef]

[18] Raaj RK, Anirudh PV, Karunakaran C, Kannan C, Jahagirdar A, Joshi S, et al. Exploring grinding and burnishing as surface post-treatment options for electron beam additive manufactured Alloy 718. Surf Coat Technol 2020;397:126063. [CrossRef]

[19] Yaman N, Sunay N, Kaya M, Kaynak Y. Enhancing Surface Integrity of Additively Manufactured Inconel 718 by Roller Burnishing Process. Procedia CIRP 2022;108:681–686. [CrossRef]

[20] Shinoda Y, Santhosh B, Palleda S, Kondo T, Kondo K, Kakehi K. Effects of substrate preheating on mechanical properties of in 718 processed by selective laser melting. SSRN 2022;4017319. [CrossRef]

[21] Yıldırım ÇV. Experimental comparison of the performance of nanofluids, cryogenic and hybrid cooling in turning of Inconel 625. Tribol Int 2019;137:366–378. [CrossRef]

[22] Taşcıoğlu E, Kaynak Y, Sharif S, Pıtır F, Suhaimi MA. Machining-induced surface integrity of Inconel 718 alloy fabricated by powder bed fusion additive manufacturing under various laser processing parameters. Mach Sci Technol 2022;26:49–71. [CrossRef]

[23] Hassan AM. The effects of ball-and roller-burnishing on the surface roughness and hardness of some non-ferrous metals. J Mater Process Technol 1997;72:385–391. [CrossRef]

[24] Kaynak Y, Tascioglu E. Finish machining-induced surface roughness, microhardness and XRD analysis of selective laser melted Inconel 718 alloy. Procedia Cirp 2018;71:500–504. [CrossRef]

[25] Hamadache H, Laouar L, Zeghib N, Chaoui K. Characteristics of Rb40 steel superficial layer under ball and roller burnishing. J Mater Process Technol. 2006;180:130–136. [CrossRef]

[26] Olugbade TO, Lu J. Literature review on the mechanical properties of materials after surface mechanical attrition treatment (SMAT). Nano Mater Sci 2020;2:3–31. [CrossRef]

[27] De Lacalle LL, Lamikiz A, Sánchez J, Arana J. The effect of ball burnishing on heat-treated steel and Inconel 718 milled surfaces. Int J Adv Manuf Technol 2007;32:958–968. [CrossRef]

[28] Vyshnepolskyi Y, Pavlenko D, Tkach D, Dvirnyk Y. Parts Diamond Burnishing Process Regimes optimization Made of INCONEL 718 Alloy via Selective Laser Sintering Method. 2020 IEEE 10th International Conference Nanomaterials: Applications & Properties (NAP). IEEE; 2020:02SAMA01-1-02SAMA01-5. [CrossRef]

[29] Grzesik W, Żak K. Producing high quality hardened parts using sequential hard turning and ball burnishing operations. Precision Eng 2013;37:849–855. [CrossRef]

[30] Kaynak Y, Karaca H, Jawahir I. Cutting speed dependent microstructure and transformation behavior of NiTi alloy in dry and cryogenic machining. J Mater Eng Perform 2015;24:452–460. [CrossRef]

[31] Kaynak Y, Tobe H, Noebe R, Karaca H, Jawahir I. The effects of machining on the microstructure and transformation behavior of NiTi Alloy. Scr Mater 2014;74:60–63. [CrossRef]

[32] Jia Q, Gu D. Selective laser melting additive manufacturing of Inconel 718 superalloy parts: Densification, microstructure and properties. J Alloys Compd 2014;585:713–721. [CrossRef]

[33] Varin RA, Czujko T, Wronski ZS. Nanomaterials for solid state hydrogen storage. Springer Science & Business Media; 2009. [CrossRef]